

REAL-TIME JOINT PERSONALIZED SPEECH ENHANCEMENT AND ACOUSTIC ECHO CANCELLATION WITH E3NET

Sefik Emre Eskimez, Takuya Yoshioka, Alex Ju, Min Tang, Tanel Pärnamaa, Huaming Wang

Microsoft, Redmond, WA, USA

{seeskime, tayoshio, aleju, mintang, taparnam, huawang}@microsoft.com

ABSTRACT

Personalized speech enhancement (PSE), a process of estimating a clean target speech signal in real time by leveraging a speaker embedding vector of the target talker, has garnered much attention from the research community due to the recent surge of online meetings across the globe. For practical full duplex communication, PSE models require an acoustic echo cancellation (AEC) capability. In this work, we employ a recently proposed causal end-to-end enhancement network (E3Net) and modify it to obtain a joint PSE-AEC model. We dedicate the early layers to the AEC task while encouraging later layers for personalization by adding a bypass connection from the early layers to the mask prediction layer. This allows us to employ a multi-task learning framework for joint PSE and AEC training. We provide extensive evaluation test scenarios with both simulated and real-world recordings. The results show that our joint model comes close to the expert models for each task and performs significantly better for the combined PSE-AEC scenario.

Index Terms— personalized speech enhancement, target speech extraction, acoustic echo cancellation, multi-task training

1. INTRODUCTION

Many institutions have adopted online communication tools for hybrid/remote work due to the COVID-19 pandemic, which has become a norm as the world transitions to the post-pandemic era. In addition, people have been relying on these tools for connecting with family members and friends. However, online communications can easily be disrupted by unwanted interference, such as other speakers in the room, background noises (TV, radio, dogs barking, babies crying, etc.), and acoustic echoes. Consequently, most online communication tools have adopted unified real-time speech enhancement (SE) and acoustic echo cancellation (AEC) methods.

A limitation of SE, AEC, and joint SE-AEC models is that they are trained to preserve all human voices that exist in the near end. Therefore, speech sounds from other speakers in the same environment (interfering speakers) can “leak” into the outbound signal, disrupting the call and compromising privacy.

Recently, personalized speech enhancement (PSE) models have attracted researchers’ attention due to their capacity to remove the interfering speech in addition to the background noise [1, 2, 3]. The PSE systems are SE systems that are conditioned on a cue from the target speaker, usually a speaker embedding vector such as a d-vector. They remove all other speakers in the input audio except for the target speaker, suppress the background noise, and apply dereverberation [2, 3]. However, most existing PSE models do not have the AEC capability. While it is desirable for a single model to encompass all of PSE, AEC, and joint PSE-AEC tasks [4, 5], it is still challenging for a real-time model to handle all these different tasks under a strict cost requirement.

This paper proposes an efficient causal joint model that can handle the PSE, AEC, and joint PSE-AEC tasks. We build upon the end-to-end enhancement network (E3Net), a recently proposed low-cost PSE model [3], by adding the AEC capacity. The proposed model incorporates the attention-based align-block described in [6] to improve the AEC performance for real recordings by softly aligning the microphone and far-end signal inputs. Furthermore, to prevent the model from becoming unduly dependent on the speaker embedding vector even for echo removal, which we have found to exacerbate undesirable target speaker over suppression (TSOS), our proposed model uses the speaker embedding vector only in the latter half of the network and introduces a bypass path during training to encourage the earlier layers to focus exclusively on the echo and near-end noise removal. This allows the later layers to focus on removing the interfering speakers and the residuals from the early layers. The model is trained with multi-task learning using three different types of mini-batches, i.e., AEC data mini-batch, PSE data mini-batch, and PSE-AEC data mini-batch, to learn all these tasks, where the bypass path is used for the AEC mini-batch. Comprehensive evaluations were carried out by using both simulated data and real recordings. The proposed model showed similar levels of performance to expert PSE and AEC models on the corresponding tasks with a similar real-time factor (RTF). Also, our model exhibited limited TSOS, which is critical for the PSE models to be accepted for real usage.

2. RELATED WORK

We define PSE as the process of extracting a clean target speech signal in real time based on a speaker embedding vector of the target talker. While the primary objective is to improve speech quality in telecommunications, we also pay attention to automatic speech recognition (ASR) accuracy since live captioning has become a popular feature in online meeting tools. The term target speech extraction (TSE) has been used almost interchangeably, and multiple TSE methods were proposed, including SpeakerBeam [7], VoiceFilter [8], and VoiceFilter-Lite [9]. However, these methods were mostly focused on ASR performance with no or limited evaluation results reported with respect to speech quality.

Several computationally efficient PSE methods can be found in the literature. Personalized PercepNet [1] modified the original PercepNet [10] by conditioning it on the speaker embedding to enhance only the target speaker. Eskimez et al. [2] proposed several PSE models, including a personalized version of deep complex convolution recurrent network (pDCCRN), and highlighted the target speaker over-suppression (TSOS) problem that arises due to the ambiguity in speaker characteristics. They proposed a metric to measure the degree of TSOS and proposed mitigation methods. Thakker et al. [3] proposed an efficient time-domain model, called a personalized E3Net. The model was shown to outperform bigger models

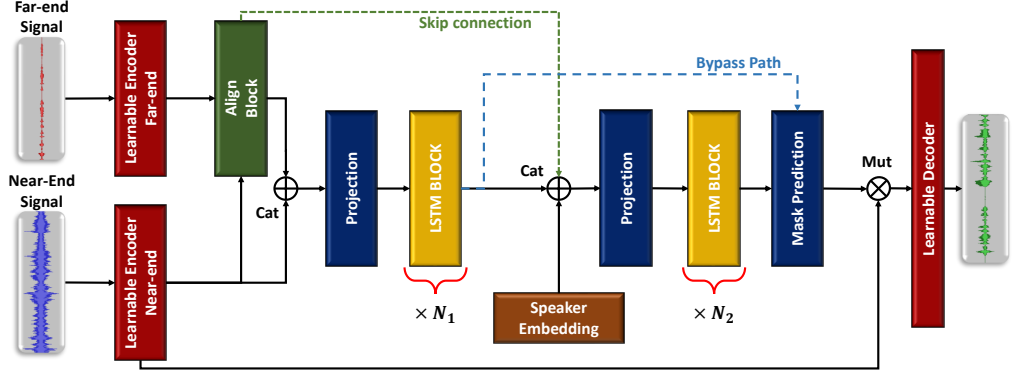


Fig. 1. The modified E3Net for PSE-AEC task. “Cat” and “Mut” stand for concatenation and element-wise multiplication, respectively.

such as pDCCRN in terms of speech quality and TSOS with a much smaller computational cost. However, all these PSE models did not address the AEC problem.

The AEC technology has been shifting from the traditional digital signal processing (DSP) approach to deep learning (DL) methods leveraging a growing amount of data [11, 12, 13]. Some studies adopted a DL and DSP hybrid approach [14, 15] while others employed DL-only methods [4, 5, 6, 11, 12, 13]. Indenbom et al. [6] proposed an attention-based soft alignment module for taking account of the potentially varying time delays between the microphone and far-end signals. The method demonstrated improvements for challenging AEC scenarios encountered in real online meetings. Yu et al. [5] proposed a self-attentive recurrent neural network-based AEC system. Although the method additionally supports speaker embedding-based personalization, it was not tested for PNS.

For joint PSE-AEC, Zhang et al. [4] recently proposed a model which can utilize the target speaker’s embedding, the far-end speaker’s embedding, or both for personalization. The model was tested only with simulated data for the scenarios where the far-end signal was always active. Therefore, its robustness in the PSE task, where only the near-end speaker is active, is unclear. Also, the model’s robustness to continuous long-form input and various distortions in real recordings was not investigated. In contrast, we carried out a comprehensive evaluation covering a wide range of scenarios, including PSE-only, AEC-only, and PSE-AEC, with both simulated data and real recordings. We also pay close attention to the computational cost, achieving a very small RTF unlike [4].

3. E3NET FOR PSE-AEC

3.1. Model Architecture

We build our system based on E3Net, an efficient causal end-to-end enhancement network [3]. Instead of relying on STFT features, E3Net utilizes a learnable encoder and decoder and predicts a mask to be applied to the learned features to achieve dereverberation, noise suppression, and interfering speaker removal. After the encoder layer, the model has a projection layer comprising non-linear activation, layer normalization, and a fully connected layer, yielding embeddings with a lower dimension f_{emb} . These embeddings are fed to a stack of N LSTM blocks, each consisting of two fully connected and non-linear activation layers followed by the first layer normalization, an LSTM, the second layer normalization, a skip connection (addition) from the first layer normalization output, and the third layer normalization. The pair of the two fully connected layers projects each embedding to a high-dimensional hidden space of dimension f_{emb_hid} and then projects it back to a f_{emb} -dimensional space. A mask prediction layer is added on top of the LSTM blocks, which consist of a fully connected layer with sigmoid activation. The

mask is applied to the features generated by the encoder. Then, the masked features are fed to the learnable decoder to produce an enhanced signal. Further details can be found in [3].

We modify the E3Net architecture as follows to cope with PSE, AEC, and PSE-AEC tasks. Fig. 1 shows the proposed architecture.

Learnable encoder: First, we add a learnable encoder for the far-end signal input. Prior PSE work [3] showed that increasing the number of learnable encoder’s filters, F_{mic} resulted in significant speech quality improvement. For the far-end signal input, a smaller number of learned features, F_{far} , can be used without impacting speech quality since the features are used only for aligning the far-end and microphone signals for echo removal.

Align-block: We use the align-block with source-target attention proposed in [6], which was shown to be particularly effective when the microphone and far-end signals were unaligned. We use the learnable features described above as the align-block input instead of the STFT features that were used in [6].

Bypass path: In the original E3Net for PSE, the speaker embedding vector is concatenated with the encoded microphone features prior to the feature projection. However, our preliminary experiment found that applying this structure to the PSE-AEC task increased TSOS when the far-end signal was not present. In PSE-AEC, both the far-end signal input and the speaker embedding vector may be used as clues for removing the echo signal. We conjecture that the observed TSOS increase was the result of the model becoming over-reliant on the speaker embedding even when the far-end signal provides sufficient clues for the echo removal, which would hurt model’s robustness. To counteract this, we append the speaker embedding vector to the N_1 th LSTM block output. Subsequently, another projection layer reduces the dimensionality of the concatenated features to the embedding’s dimension and feeds them to the remaining N_2 LSTM blocks. This architectural change is aimed at dedicating the earlier LSTM blocks to the AEC task. To further encourage the first N_1 LSTM blocks to focus on AEC, we add a path bypassing the later N_2 LSTM blocks (the blue dashed line in Fig. 1) and perform multi-task learning by using AEC-NS training samples (see Section 3.2).

Skip connection: Lastly, we append the attention weights from the align-block to the N_1 th LSTM block output to help the latter LSTM blocks adjust the noise suppression behavior based on the presence of the echo signal.

3.2. Multi-Task Training

Our joint model aims to be as effective as task-specific models for AEC and PSE while outperforming the task-specific models in the PSE-AEC task where the target speaker, interfering speakers, acoustic echo, and near-end noise simultaneously exist in the microphone signal. To this end, we consecutively use three mini-batches with

Table 1. Experimental results for PSE and PSE-AEC using VCTK and VCTK-AEC data sets, respectively, each consisting of three test scenarios. TS1 includes the target, interfering speaker, and noise. TS2 includes the target speaker and noise. TS3 includes only the target speaker. All scenarios include reverberation. Far-end signals are inactive in VCTK and active in VCTK-AEC.

| VCTK | | | | | | | | |
|-----------------------|--------------|-------------|--------------|--------------|--------------|--------------|--------------|--------------|
| | TS1 | | | TS2 | | | TS3 | |
| | WER↓ | DNSMOS↑ | TSOS↓ | WER↓ | DNSMOS↑ | TSOS↓ | WER↓ | TSOS↓ |
| No Enhancement | 43.03 | 2.92 | 0 | 13.35 | 2.98 | 0 | 7.12 | 0 |
| AlignCruse | 57.10 | 3.27 | 0 | 21.82 | 3.41 | 0 | 7.47 | 0 |
| AEC E3Net | 43.50 | 3.51 | 0.33 | 18.05 | 3.71 | 0.17 | 7.19 | 0.05 |
| PSE E3Net | 36.91 | 3.49 | 2.15 | 18.35 | 3.74 | 0.33 | 7.54 | 0.32 |
| PSE-AEC E3Net | | | | | | | | |
| - Naïve | 38.70 | 3.47 | 1.54 | 19.76 | 3.70 | 0.96 | 7.82 | 1.38 |
| - w/o skip connection | 38.96 | 3.43 | 1.45 | 19.43 | 3.68 | 0.51 | 7.46 | 0.06 |
| - w/ skip connection | 38.05 | 3.48 | 1.62 | 19.76 | 3.71 | 0.52 | 7.45 | 0.14 |
| VCTK-AEC | | | | | | | | |
| | TS1 | | | TS2 | | | TS3 | |
| | WER↓ | DNSMOS↑ | AECMOS ECHO↑ | WER↓ | DNSMOS↑ | AECMOS ECHO↑ | WER↓ | AECMOS ECHO↑ |
| No Enhancement | 54.78 | 1.18 | 2.42 | 0.0 | 33.10 | 2.0 | 2.37 | 0.0 |
| AlignCruse | 62.46 | 2.39 | 3.53 | 0.04 | 37.29 | 2.58 | 3.85 | 0.04 |
| AEC E3Net | 58.19 | 2.80 | 4.26 | 0.14 | 30.12 | 3.06 | 4.48 | 0.18 |
| PSE E3Net | 51.40 | 2.69 | 4.23 | 1.09 | 33.51 | 2.95 | 4.41 | 0.63 |
| PSE-AEC E3Net | | | | | | | | |
| - Naïve | 54.06 | 2.64 | 4.24 | 0.83 | 33.85 | 2.87 | 4.39 | 0.22 |
| - w/o skip connection | 51.88 | 2.63 | 4.27 | 0.82 | 32.70 | 2.91 | 4.46 | 0.46 |
| - w/ skip connection | 49.97 | 2.75 | 4.35 | 1.07 | 31.08 | 2.98 | 4.48 | 0.46 |
| | | | | | | | 18.70 | 4.50 |
| | | | | | | | 18.33 | 4.54 |
| | | | | | | | 17.16 | 4.56 |
| | | | | | | | | 0.15 |

different data configurations during training.

AEC mini-batch—which contains the target speaker, near-end noise, and echo signals. These samples do not include speaker embedding vectors. Hence, the model uses the bypass path to encourage the earlier LSTM blocks to focus on AEC and noise suppression.

PSE mini-batch—which includes the target and interfering speakers as well as noise. The speaker embedding vectors are included, while the far-end signal is all-zero. The full path of the model is trained. The PSE mini-batch helps the model learn the PSE capability.

PSE-AEC mini-batch—which includes all signals as well as the speaker embedding vectors. The model uses the full path. This mini-batch helps the model learn to jointly perform PSE and AEC. It also improves full-path AEC quality by exposing the later LSTM blocks to training samples with non-zero echo signals.

4. EXPERIMENTAL RESULTS

4.1. Training, Validation, and Test Data

We simulated PSE training and validation data by using the same configuration as used in [2, 3]. The clean speech utterances needed for the simulation were taken from the DNS challenge data [16]. The data set is based on LibriVox recordings [17] and contains 544 hours of speech samples. We used noise samples from the AudioSet [18] and Freesound [19] data sets. For each training and validation sample, we randomly placed the target speaker between 0 to 1.3 meters away from the microphone, and the interfering speaker more than 2 meters away by using simulated room impulse responses (RIRs). Only half of the samples included interfering speakers to improve the model’s SE task performance. The signal-to-noise ratio (SNR) and signal-to-interference ratio (SIR) were varied from 0 to 15 dB and from 0 to 10 dB, respectively. The clean speech source for the echo signal was obtained from the DNS challenge [16], which includes singing and emotional speech. We also employed RIRs, additive noise, and distortion models for the echo simulation.

For PSE evaluation, we used the simulated long-duration test sets of [2, 3] based on the voice cloning toolkit (VCTK) corpus [20]. The test sets cover three important near-end signal scenarios: **TS1**:

target speaker + interfering speaker + noise, **TS2**: target speaker + noise, and **TS3**: target speaker only. TS1 and TS2 measure the model performance in the PSE and SE scenarios, respectively, while TS3 is for target speaker degradation assessment. VCTK was used as the clean speech source. The files from the same speaker were stitched together to create a single long-duration file per speaker. Therefore, the acoustic conditions (interfering speaker, noise, RIR, SNR, and SIR) change every few seconds, making this a challenging evaluation set. The average duration of the individual test samples was 27.5 minutes. In addition, we also evaluated our models on the DNS challenge personalized track [16], which consists of real recordings, including interfering speakers.

We tested our AEC performance on the blind test set of the ICASSP 2022 AEC Challenge [13]. This test set consists of 600 real-world recordings of 30-45 seconds each, which are split equally into far-end single-talk (FST) and double-talk (DT) cases. Furthermore, this test set includes challenging scenarios commonly found in real online meetings: long and varying delays between microphone and far-end signals, loudspeaker and microphone distortions, non-stationary noise, echo path changes due to moving near-end speakers, audio DSP processing artifacts, and gain variations [13].

To test the PSE-AEC scenario, we modified the aforementioned simulated VCTK PSE test sets [2, 3]. Far-end speaker signals were selected from the VCTK corpus by excluding the target speaker. These samples were stitched to the length of each PSE test sample and convolved with a random RIR. Distortions such as sigmoidal squashing, clipping, and glitches (such as jitter) were added, and the echo signals were mixed into the PSE test set with a signal-to-echo ratio (SER) between -2.5 and 15 dB. We refer to this modified VCTK test set as the VCTK-AEC test set.

4.2. Evaluation Metrics and Implementation Details

We measured the automatic speech recognition (ASR) quality, speech quality, and target speaker over-suppression (TSOS) for PSE evaluation. Specifically, we used DNSMOS P.835 [21], which is a neural network-based mean opinion score (MOS) estimator predicting subjective quality ratings with high accuracy, to measure

Table 2. Computational complexities of different models and their results for real recording test sets. RTF was measured on Intel(R) Xeon(R) W-2133 CPU @ 3.60GHz with a single-thread configuration by taking averages over 100 independent runs.

| | Real-world Recordings | | | | | | | | |
|-----------------------|-----------------------|-------|---------------|-------------|-------------|-------------------|--------------|------------------|-------------|
| | Complexity | | DNS Challenge | | | AEC Challenge FST | | AEC Challenge DT | |
| | Parameters (millions) | RTF | SIG↑ | BAK↑ | OVR↑ | AECMOS ECHO↑ | ERLE↑ | AECMOS ECHO↑ | AECMOS DEG↑ |
| No Enhancement | - | - | 3.71 | 2.17 | 2.40 | 1.98 | 0.0 | 1.81 | 4.11 |
| AlignCruse | 0.45 | 0.056 | 3.58 | 3.85 | 3.18 | 4.12 | 44.40 | 4.34 | 3.91 |
| AEC E3Net | 3.3 | 0.054 | 3.52 | 4.09 | 3.24 | 4.47 | 47.91 | 4.65 | 3.97 |
| PSE E3Net | 3.2 | 0.050 | 3.53 | 4.07 | 3.24 | 2.20 | 11.42 | 4.33 | 4.04 |
| PSE-AEC E3Net | | | | | | | | | |
| - Naïve | 3.3 | 0.054 | 3.49 | 4.06 | 3.19 | 4.39 | 45.38 | 4.61 | 3.46 |
| - w/o skip connection | 3.3 | 0.054 | 3.45 | 4.08 | 3.16 | 4.45 | 49.06 | 4.61 | 3.92 |
| - w/ skip connection | 3.3 | 0.054 | 3.52 | 4.09 | 3.23 | 4.41 | 46.78 | 4.62 | 3.98 |

speech quality. Microsoft’s internal ASR model was used to obtain the word error rate (WER). In addition, we calculated the target speaker over suppression metric of [2]. We measured the AEC quality using AECMOS [22], a neural network mean opinion score (MOS) estimator, which is similar to DNSMOS but was developed for measuring the echo removal quality (AECMOS ECHO) and signal degradation (AECMOS DEG). Echo return loss enhancement (ERLE) was also used for the FST scenario. For real data without clean reference signals, namely the DNS and AEC challenge test sets, DNSMOS and AECMOS were used, respectively.

Both training and validation samples were 20 seconds long. We set the f_{emb} and f_{emb_hid} to 128 and 768, respectively. The input and hidden dimensions of the LSTM blocks were the same and set to f_{emb} . The learnable encoder and decoder window (filter size) and hop size (stride) were 20 ms (320) and 10 ms (160), respectively. The dimensions of the learnable encoders for the microphone and far-end signals, F_{mic} and F_{far} , were 2048 and 256, respectively. The number of the LSTM blocks, N_1 and N_2 , were both 2, totaling to 4 LSTM blocks as with the original E3Net. Baseline E3Net training followed the aforementioned parameters and used 4 LSTM blocks. We trained all the models with the power-law compressed phase-aware (PLCPA) loss function (see Eq. (1) of [2]).

4.3. Baseline Models

We chose AlignCruse of [6] as our baseline model for the AEC task. AlignCruse is an STFT-based model that includes an encoder, decoder, and align-block. The encoder and decoder contain 2D convolutional layers that gradually reduce the spectrogram dimensions. AlignCruse has GRU layers in the bottle-neck. It showed promising results in the AEC task with a similar computational cost to E3Net. We used the authors’ code and pre-trained model, which outperformed the one reported in the original paper [6]. In addition, for the AEC task, we trained an AEC E3Net model with the same architecture as the PSE-AEC E3Net model. Note that some training noise files might have contained human speech, potentially leading to the AEC E3Net model having a modest interfering speaker suppression capability. For the PSE baseline, we used a personalized E3Net almost identical to the original model. We changed the hyperparameters to match that of the PSE-AEC E3Net model. A PSE-AEC E3Net-Naïve model was also trained to provide a PSE-AEC baseline by directly using the PSE E3Net architecture. It uses the learnable encoder for both the microphone and far-end signals and concatenates these features and the speaker embedding vector before the projection layer. The naïve model does not contain the align-block, the proposed bypass path, and the second projection layer.

4.4. Results and Discussions

Tables 1 and 2 show the results for the simulated and real-world recordings test sets, respectively. First, we compare the baseline

models, i.e., AlignCruse, AEC E3Net, and PSE E3Net. AEC and PSE E3Net perform better than AlignCruse in the simulated test sets and real-world recordings for all scenarios. As expected, AEC E3Net underperforms the PSE E3Net for the TS1 scenario (for both VCTK and VCTK-AEC) since AEC E3Net has little interfering speaker suppression capability. AEC and PSE E3Net perform similarly for VCTK TS2 and TS3 scenarios, but PSE E3Net performs worse on VCTK-AEC TS2 and TS3 scenarios, as expected. It should be noted that PSE E3Net was not trained to remove the echo, but it has an inherent capability to remove echo due to personalization. This is validated in Table 2, where PSE E3Net and AlignCruse have similar results for the DT scenario. However, the PSE E3Net model can get confused and lock to the wrong speaker if there is no target speaker in the recording, hence low scores in the FST scenario.

Next, we compare the joint PSE-AEC models. Table 1 shows that the PSE-AEC-naïve model has higher TSOS, especially for TS2 and TS3. In addition, Table 2 shows that the naïve model has a lower AECMOS DEG score than the other models, suggesting high distortion for the double-talk case. In contrast, the joint models with and without skip connection perform much better in the double-talk case and have higher AECMOS ECHO and DEG scores compared to the AlignCruse baseline and similar scores to the AEC E3Net expert model. Furthermore, VCTK and VCTK-AEC results suggest they perform similarly to the expert PSE and AEC E3Net models. Using the skip connection for the joint model slightly improves the DNSMOS and AECMOS DEG at the cost of FST performance for the real-world recordings and yields lower WER for the simulated ones, especially for VCTK-AEC. According to the results, we can draw the following conclusions: 1) Our modifications (multi-task training, bypass path, and align-block) improve the results for both PSE and AEC tasks for E3Net over the naïve model, 2) AEC E3Net performs better than the AlignCruse model, which has a similar computational cost, 3) Our joint model performs similarly to the expert AEC and PSE models, 4) Adding the skip connection improves the signal quality slightly.

5. CONCLUSIONS

We proposed a joint PSE-AEC system trained with a multi-task learning framework in this work. We modified the end-to-end enhancement network (E3Net) for both AEC and PSE tasks, including adding a new learnable encoder for the far-end signal, an align-block for better AEC performance, and a bypass path to enable multi-task learning. We evaluated our joint model in various test sets that cover multiple scenarios for AEC and PSE tasks using both long-duration simulation data and real-world recordings. The results showed that the joint model performance was similar to the PSE and AEC expert models in the PSE and AEC tasks, respectively. Furthermore, the joint model performed significantly better in the PSE-AEC task.

6. REFERENCES

- [1] R. Giri, S. Venkataramani, J.-M. Valin, U. Isik, and A. Krishnaswamy, “Personalized PercepNet: Real-Time, Low-Complexity Target Voice Separation and Enhancement,” in *Proc. INTERSPEECH*, 2021, pp. 1124–1128.
- [2] S. E. Eskimez, T. Yoshioka, H. Wang, X. Wang, Z. Chen, and X. Huang, “Personalized speech enhancement: new models and comprehensive evaluation,” in *Proc. ICASSP*, 2022, pp. 356–360.
- [3] M. Thakker, S. E. Eskimez, T. Yoshioka, and H. Wang, “Fast Real-time Personalized Speech Enhancement: End-to-End Enhancement Network (E3Net) and Knowledge Distillation,” in *Proc. INTERSPEECH*, 2022, pp. 991–995.
- [4] S. Zhang, Z. Wang, Y. Ju, Y. Fu, Y. Na, Q. Fu, and L. Xie, “Personalized acoustic echo cancellation for full-duplex communications,” *arXiv preprint arXiv:2205.15195*, 2022.
- [5] M. Yu, Y. Xu, C. Zhang, S.-X. Zhang, and D. Yu, “Neuralecho: A self-attentive recurrent neural network for unified acoustic echo suppression and speech enhancement,” *arXiv preprint arXiv:2205.10401*, 2022.
- [6] E. Indenbom, N.-C. Ristea, A. Saabas, T. Pärnamaa, and J. Gužvin, “Deep model with built-in self-attention alignment for acoustic echo cancellation,” *arXiv preprint arXiv:2208.11308*, 2022.
- [7] M. Delcroix, T. Ochiai, K. Zmolikova, K. Kinoshita, N. Tawara, T. Nakatani, and S. Araki, “Improving speaker discrimination of target speech extraction with time-domain speakerbeam,” in *Proc. ICASSP*, 2020, pp. 691–695.
- [8] Q. Wang, H. Muckenhirk, K. Wilson, P. Sridhar, Z. Wu, J. R. Hershey, R. A. Saurous, R. J. Weiss, Y. Jia, and I. L. Moreno, “VoiceFilter: Targeted Voice Separation by Speaker-Conditioned Spectrogram Masking,” in *Proc. INTERSPEECH*, 2019, pp. 2728–2732.
- [9] Q. Wang, I. L. Moreno, M. Saglam, K. Wilson, A. Chiao, R. Liu, Y. He, W. Li, J. Pelecanos, M. Nika, and A. Gruenstein, “VoiceFilter-Lite: Streaming Targeted Voice Separation for On-Device Speech Recognition,” in *Proc. INTERSPEECH*, 2020, pp. 2677–2681.
- [10] J.-M. Valin, U. Isik, N. Phansalkar, R. Giri, K. Helwani, and A. Krishnaswamy, “A Perceptually-Motivated Approach for Low-Complexity, Real-Time Enhancement of Fullband Speech,” in *Proc. INTERSPEECH*, 2020, pp. 2482–2486.
- [11] K. Sridhar, R. Cutler, A. Saabas, T. Pärnamaa, M. Loide, H. Gamper, S. Braun, R. Aichner, and S. Srinivasan, “Icassp 2021 acoustic echo cancellation challenge: Datasets, testing framework, and results,” in *Proc. ICASSP*, 2021, pp. 151–155.
- [12] R. Cutler, A. Saabas, T. Pärnamaa, M. Loide, S. Sootla, M. Purin, H. Gamper, S. Braun, K. Sørensen, R. Aichner, and S. Srinivasan, “INTERSPEECH 2021 Acoustic Echo Cancellation Challenge,” in *Proc. INTERSPEECH*, 2021, pp. 4748–4752.
- [13] R. Cutler, A. Saabas, T. Pärnamaa, M. Purin, H. Gamper, S. Braun, K. Sørensen, and R. Aichner, “Icassp 2022 acoustic echo cancellation challenge,” in *Proc. ICASSP*, 2022, pp. 9107–9111.
- [14] J. Casebeer, N. J. Bryan, and P. Smaragdis, “Auto-dsp: Learning to optimize acoustic echo cancellers,” in *Proc. WASPAA*, 2021, pp. 291–295.
- [15] L. Ma, H. Huang, P. Zhao, and T. Su, “Acoustic echo cancellation by combining adaptive digital filter and recurrent neural network,” *arXiv preprint arXiv:2005.09237*, 2020.
- [16] H. Dubey, V. Gopal, R. Cutler, A. Aazami, S. Matusevych, S. Braun, S. E. Eskimez, M. Thakker, T. Yoshioka, H. Gamper *et al.*, “Icassp 2022 deep noise suppression challenge,” in *Proc. ICASSP*, 2022, pp. 9271–9275.
- [17] J. Kearns, “Librivox: Free public domain audiobooks,” *Reference Reviews*, 2014.
- [18] J. F. Gemmeke, D. P. W. Ellis, D. Freedman, A. Jansen, W. Lawrence, R. C. Moore, M. Plakal, and M. Ritter, “Audio set: An ontology and human-labeled dataset for audio events,” in *Proc. ICASSP*, 2017, pp. 776–780.
- [19] E. Fonseca, J. Pons, X. Favory, F. Font, D. Bogdanov, A. Ferraro, S. Oramas, A. Porter, and X. Serra, “Freesound datasets: A platform for the creation of open audio datasets,” in *Proc. ISMIR*, 2017, pp. 486–493.
- [20] V. Christophe, Y. Junichi, and M. Kirsten, “Cstr vctk corpus: English multi-speaker corpus for cstr voice cloning toolkit,” *The Centre for Speech Technology Research (CSTR)*, 2016.
- [21] C. K. Reddy, V. Gopal, and R. Cutler, “Dnsmos p. 835: A non-intrusive perceptual objective speech quality metric to evaluate noise suppressors,” *arXiv preprint arXiv:2110.01763*, 2021.
- [22] M. Purin, S. Sootla, M. Sponza, A. Saabas, and R. Cutler, “Aecmos: A speech quality assessment metric for echo impairment,” in *Proc. ICASSP*, 2022, pp. 901–905.